

## **PCTFE as a solution to birefringence in atom trap viewports**

C. L. Warner, J. A. Behr, and A. Gorelov

Citation: [Review of Scientific Instruments](#) **85**, 113106 (2014); doi: 10.1063/1.4900957

View online: <http://dx.doi.org/10.1063/1.4900957>

View Table of Contents: <http://scitation.aip.org/content/aip/journal/rsi/85/11?ver=pdfcov>

Published by the [AIP Publishing](#)

---

### **Articles you may be interested in**

[A density functional theory study of magneto-electric Jones birefringence of noble gases, furan homologues, and mono-substituted benzenes](#)

J. Chem. Phys. **139**, 194311 (2013); 10.1063/1.4830412

[Modeling of Crystallization, Birefringence and Anisotropic Shrinkage in Injection Molding of Thermoplastics](#)

AIP Conf. Proc. **712**, 216 (2004); 10.1063/1.1766526

[Diffusion of hydrogen in rare gas solids: neutral H atoms and H + protons](#)

Low Temp. Phys. **25**, 814 (1999); 10.1063/1.593823

[Flow-Induced Birefringence of Concentrated Polyisoprene Solutions](#)

J. Rheol. **33**, 517 (1989); 10.1122/1.550026

[A Method for Determining Diffusion Constants of Colloids which Show Mechanical Birefringence](#)

J. Rheol. **3**, 494 (1932); 10.1122/1.2116511

---



## PCTFE as a solution to birefringence in atom trap viewports

C. L. Warner,<sup>1,2,a)</sup> J. A. Behr,<sup>1</sup> and A. Gorelov<sup>1</sup>

<sup>1</sup>TRIUMF, Canada's National Lab for Particle and Nuclear Physics, 4004 Wesbrook Mall, Vancouver, British Columbia V6T 2A3, Canada

<sup>2</sup>Department of Physics and Astronomy, University of Waterloo, 200 University Avenue West, Waterloo, Ontario N2L 3G1, Canada

(Received 27 August 2014; accepted 21 October 2014; published online 11 November 2014)

We have developed and characterized optical viewports with the glass-to-metal seal made by the plastic PCTFE (polychlorotrifluoroethylene). The goal is to reduce stress-induced birefringence while maintaining ultra-high vacuum compatibility. We have maintained a Stokes parameter  $S_3$  of 0.9986, and achieved  $<5 \times 10^{-11}$  Torr partial pressure of air. We have also measured the diffusion and permeation of helium through PCTFE and placed upper limits on nitrogen, oxygen, and argon permeation, as PCTFE has been suggested as an o-ring for transport of environmental noble gas samples, though we know of no other noble gas measurements. © 2014 AIP Publishing LLC. [<http://dx.doi.org/10.1063/1.4900957>]

### I. INTRODUCTION

At TRIUMF's Neutral Atom Trap (TRINAT), one current goal is a measurement of the angular asymmetry of beta particles with respect to the nuclear spin,  $A_\beta$ , from the beta decay of spin-polarized  $^{37}\text{K}$  nuclei.<sup>1</sup> The atoms and nuclei are polarized by optical pumping with circularly polarized light. The experimentally measured quantity is  $P \times A_\beta$ , where the nuclear polarization  $P$  achieved depends on the quality of circularly polarized light.

One major difficulty in creating circularly polarized light with small ellipticity is stress-induced birefringence on the viewports of the atom trap. Using commercially welded conflat viewports assembled with fully annealed copper gaskets, we have found a small degree of birefringence that was difficult to reproducibly minimize. As an alternative to interesting solutions in the literature using indium<sup>4</sup> and combinations of solder and UHV compatible epoxy,<sup>5</sup> we discuss here our use of elastomer o-rings to make the glass to metal seal.

We have found a solution with PCTFE (polychlorotrifluoroethylene) o-rings, which provided a compromise of stress-relief and sealing which made our viewports suitable for UHV. PCTFE (trade names KEL-F and Daikin Neoflon) is known from the literature to have almost no outgassing of water and other condensables.<sup>2</sup> A wide range of permeation rates for air through PCTFE is reported in the literature (see Table I), and though the rates appear promisingly small we needed to characterize them as well. PCTFE has the disadvantage of being less deformable and pliable than common o-ring materials like FKM (fluoroelastomer, "Viton") and FFKM (perfluoroelastomer, "Kalrez"), which we compare in our geometry. PCTFE is known to be more deformable and pliable than PEEK (polyetheretherketone), another plastic with good outgassing properties that has been used for CF gaskets.<sup>3</sup>

We can characterize the viewports by their birefringence,  $\Delta n$  (Ref. 4) and we further understand the birefringence by

demonstrating the relationship between the Stokes parameter  $S_3$  and  $\Delta n$  for circularly polarized light.

$S_3$  is defined as

$$S_3 = \sqrt{1 - \left( \frac{I_{\max} - I_{\min}}{I_{\max} + I_{\min}} \right)^2}. \quad (1)$$

Ref. 4 relates  $\Delta n$  and the extinction ratio for linearly polarized light as

$$\frac{I_{\min}}{I_{\max} + I_{\min}} = \frac{1}{2}(1 - \cos(kL\Delta n + \phi)), \quad (2)$$

where  $k$  is the wave number  $\frac{1}{\lambda}$  and  $L$  is the thickness of the glass. In the case of linearly polarized light,  $\phi$  can be considered zero. However, for circularly polarized light  $\phi$  is  $\frac{\pi}{2}$ .

Therefore for circularly polarized light we can define

$$S_3 = \sin\left(kL\Delta n + \frac{\pi}{2}\right) = \cos(kL\Delta n). \quad (3)$$

This equation gives the effect on perfectly circularly polarized light of a single viewport with birefringence  $\Delta n$ .  $S_3$  varies from our goal of unity quadratically with the small quantity  $\Delta n$ , in contrast with the linear dependence on small  $\Delta n$  of linearly polarized light.<sup>4</sup> Two viewports of a vacuum system will then add their birefringence quadratically, depending as well on the relative orientation of their fast and slow axes, making it challenging to interpret results made from outside the vacuum.

We do not relate the complexity of the full optical pumping treatment and coupling to nuclear angular momentum<sup>6</sup> here. We summarize that  $S_3$  is related to the desired nuclear polarization by

$$P \approx \frac{1 + S_3}{2}, \quad (4)$$

so, for example,  $S_3$  of 0.998 is needed for  $P$  to be 0.999.

### II. O-RING VIEWPORT DESIGN

We modified a commercial viewport (Accu-Glass Products, Inc. part number 112666), a 2.75" CF flange with an

<sup>a)</sup>Electronic mail: cwerner@uwaterloo.ca

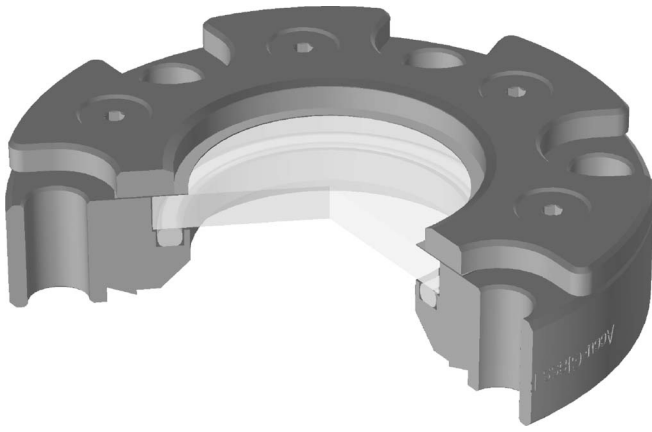


FIG. 1. Commercial viewport modified with PCTFE o-ring, 0.13 mm kapton film, and titanium screws. The PCTFE deforms so a 1.5 mm wide surface is in contact with the metal, leaving a 0.05–0.15 mm gap between the stainless steel and aluminum surfaces that simplifies interpretation of helium leak-checking.

inlaid o-ring groove. The o-ring in the groove supports the fused silica viewport (650–1050 nm anti-reflection coated) which is compressed onto the o-ring by an aluminum plate and six Grade 5 titanium 6–32 screws (Fig. 1). The titanium screws reduced friction to keep the small applied torque uniform, both between the screw and the surface and when the fastening tool was removed, and also were nonmagnetic. First  $\frac{1}{4}$ -28 bolts at 96 in.-lbs sealed the CF to the rest of the system with standard fully annealed copper gaskets, then to minimize the stress the 6–32 screws were carefully tightened to between 6 and 10 in.-lbs for PCTFE and 15 in.-lbs for FKM and FFKM.

### A. FKM and FFKM O-rings

FKM (fluoroelastomer, “Viton”) and FFKM (perfluoroelastomer, “Kalrez”) o-rings provided excellent stress relief for the viewports. The  $S_3$  values from light passed through the viewports were consistently above 0.9998. FKM and/or FFKM were not pursued as solutions because their gas permeation rates are known to be undesirably high when the goal is UHV. However it should be noted that when a helium leak check and rate of rise test were performed, we believe that FKM could be considered a viable alternative to PCTFE for a limited number of viewports, depending on the vacuum desired. We did achieve  $3 \times 10^{-8}$  torr with one FKM and one FFKM viewport in a small unbaked ion-pumped system, which can be regarded as an upper limit on what could be achieved from these materials; given other data from the literature (see Table I), this was possibly dominated by permeation through the FFKM o-ring.

### B. PCTFE O-rings

The viewports used standard o-ring size -124 PCTFE o-rings machined from compression-molded Daikin Neoflon M-400H grade material by external manufacturers. They were assembled in a clean room. Before assembly, the o-rings were inspected under a microscope for imperfections, then ultrasounded for 30 min in deionized water to remove any residual

oil or dust from the manufacturing and inspection processes. When we started using PCTFE, we used the same torque on the screws as we had used with the FKM/FFKM (15 in.-lbs). This resulted in high levels of birefringence (in some instances  $S_3$  was reduced to 0.98) and breaking two viewports. To resolve this we started to use torques for the 6–32 screws between 4 and 10 in.-lbs, with the best compromise between leaking and stress-relief occurring at 6–8 in.-lbs. We also added a ring (OD = 1.8”, ID = 1.2”) of 0.13 mm thick Kapton film to cushion the viewport against the aluminum plate holding it in place. Less torque can and should be used for the PCTFE to achieve similar sealing pressure, because it deforms less than FKM/FFKM, and so its sealing surface has smaller area (see Fig. 1). The force applied to the center of the viewport by the 6–32 screws is then typically 1/6 that of the conflat bolts, reducing the known source of stress-induced birefringence from non-uniform pressure.<sup>7</sup>

To try to guarantee a better sealing surface, we also tried polishing several o-rings before ultrasounding with  $0.3 \mu\text{m}$  aluminum oxide powder in water on a polishing cloth. This did not improve the stress-relieving quality of the o-ring, as the  $S_3$  values were not as good as when the o-rings that had not been polished were used, so polished o-rings were not used on the final system. Possible reasons for this degradation include nonuniform o-ring thickness after polishing, as well as the potential for hardening of the surface of the o-ring during polishing, either of which would put more stress on the viewport for a given torque.

## III. MEASURING $S_3$

The test setup consisted of a 1.1 mW 770 nm laser beam following a straight path through a linear polarizer, a Liquid Crystal Variable Retarder (LCVR) acting as a  $\frac{\lambda}{4}$  or  $\frac{3\lambda}{4}$  plate, the viewports, a rotating analyzing polarizer, and finally a power meter. When the analyzing polarizer is placed before the viewports, it indicates the “baseline”  $S_3$  value, while if it is placed after the viewports, the impact of the viewports on  $S_3$  can be evaluated. The angle of the primary polarizer optical axis with respect to the LCVR is crucial, especially since the optimum angle for each handedness of light was found to be slightly different. The best angle to use is between the two optimum angles for a compromise between the handednesses.

### A. Position dependence

Beams of diameter 2 mm and 12 mm were used. The 2 mm beam could be rastered across the window. The atom trap cloud to be optically pumped is a few mm in diameter.

For both the PCTFE and the FKM/FFKM, we found that the light was not affected very much by shifting the beam off-center on the viewports. When we moved the beam 6 mm off center in the case of PCTFE, the magnitude of the difference in  $\Delta n$  between a centered and un-centered beam was just  $3.4 \times 10^{-7}$ .

### B. Measuring $S_3$ on the main system

On the main vacuum system designed for  $\beta$ -decay measurements,<sup>1</sup> measuring the  $S_3$  value was slightly more

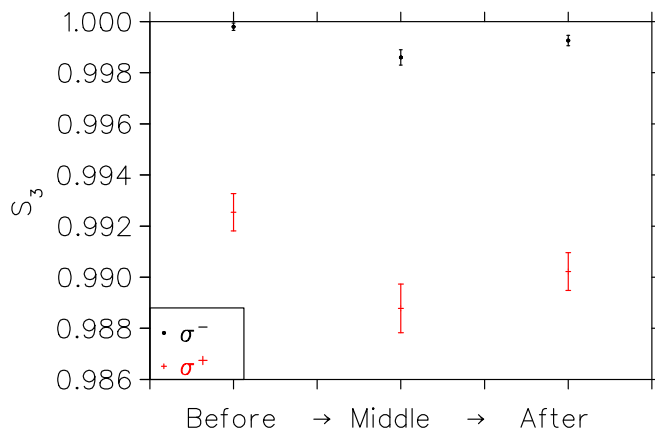


FIG. 2. Measured  $S_3$  values on main system (pre-bakeout) for each handedness of light, with light shining through from top to bottom. Note that one handedness appears to be affected much more by the viewport, because the initial  $S_3$  value is further from unity, and varies quadratically with  $\Delta n$ .

complicated. The light could either be shone through the top viewport, or through the bottom. The analyzing polarizer would then be rotated on the other side of the chamber. Before baking, we measured the  $S_3$  in the middle of the chamber (light traveling from top to bottom) and from that deduced the  $\Delta n$  contributions from each viewport using Eq. (3). In retrospect, there is information about viewport fast and slow axes for non-ideal  $S_3$  contained in the analysis angles where minimum and maximum was observed. This could in principle be used in future studies if better knowledge of  $S_3$  were needed at chamber center by combining  $\Delta n$  from the two viewports (Fig. 2).

We found at our level of accuracy that pumping the viewports rarely changed  $S_3$  significantly from the values produced by the torque of the screws.

#### IV. VACUUM ACHIEVED WITH PCTFE VIEWPORTS

To measure the vacuum we achieved with the PCTFE viewports, we combined simple rate of rise tests, helium leak rates as a function of time as the gaskets saturated in an atmosphere of helium, and partial pressures in our final vacuum system with a residual gas analyzer (RGA) and known pumping speeds. We also compare with measurements on FKM and FFKM.

##### A. Rate of rise test

To make sure that the viewports did not leak at a rate that would affect the vacuum, a rate of rise test was performed. A small vacuum system with volume 0.25 l and with two viewports was pumped to approximately 5 mTorr and sealed, while the pressure was monitored for 8–12 h. The result was fit for a leak (pressure rising linearly with time) and outgassing (a saturating exponential). The leak rate achieved with the two viewports that would be used on the final system was approximately 0.2 mTorr/h, which would extrapolate to an estimated pressure of  $1.5 \times 10^{-10}$  Torr in the final vacuum chamber. We achieved final partial pressures for air of about 1/3 these estimates (see Subsection IV B 3).

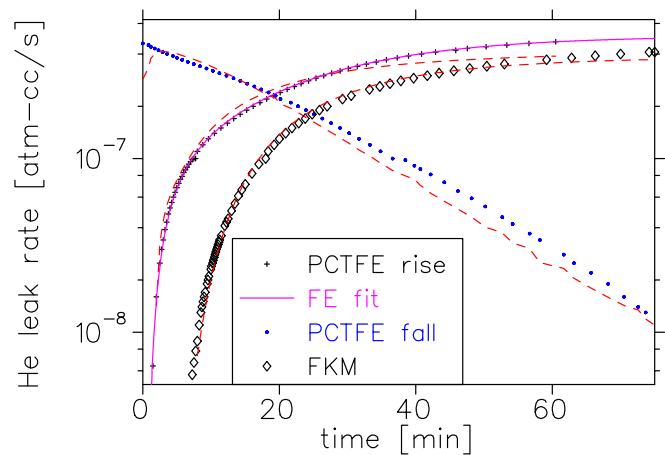


FIG. 3. Helium leak rate rise and fall of PCTFE and rise in FKM, fit to solutions of diffusion equation. Dashed red curves are Eqs. (5)–(7), solid magenta curve is a finite element calculation of the PCTFE deformed geometry (see text).

#### B. Permeation of helium and other gases

To investigate the helium permeation of PCTFE, the viewports were surrounded with helium at atmospheric pressure and the leak rate of the helium in  $\text{atm} \cdot \text{cc} \cdot \text{s}^{-1}$  was measured (Fig. 3). The leak rate very reproducibly rose to a steady equilibrium, at which point the helium source was removed. Then, the leak rate decreased as the helium which had saturated within the o-ring dissipated into the vacuum. We repeated this measurement for welded conflat viewports, which showed no helium leak, implying that permeation rates of helium through fused silica were negligibly small.

A similar measurement surrounded the viewports with an atmosphere of argon, and no leak registered on a RGA after an hour, and with no change in nitrogen or oxygen.

##### 1. Solutions of the diffusion equation

The gas flux (equivalent to leak rate) through a two-dimensional membrane of thickness  $d$  and area  $A$  exposed to pressure  $P_o$  while the membrane is in the process of saturating from a source is Ref. 11

$$F(x = d, t) = \frac{ADSP_o}{d} \left( 1 + 2 \sum_{n=1}^{\infty} (-1)^n \exp \left[ -\frac{Dn^2\pi^2 t}{d^2} \right] \right) \quad (5)$$

in terms of the diffusion coefficient  $D$  and the solubility constant  $S$ .

The limit of the leak rate after the membrane has saturated is then

$$R_{\infty} = \frac{ADSP_o}{d} \quad (6)$$

which implies that the permeation constant  $K = D \times S$  depends only on the final leak rate and not the details of the time dependence.



TABLE I. Diffusion parameters for gases in PCTFE (compression molded), FKM (Viton), and FFKM (Kalrez 4079). Present work for He shown with errors are from fits of the time dependence and saturation of helium leak rates. Present work's upper limits for N<sub>2</sub>, O<sub>2</sub>, and Ar are from the best partial pressures reached in a vacuum system with RGA and known pumping speeds. Values compiled in Ref. 8 from several sources at temperatures 20°–30°C are shown as ranges for comparison, while the values from the industrial table Ref. 9 at 30°C are quoted there as single two-digit numbers without errors. All present measurements were at room temperature.

		$D \times 10^6$ cm <sup>2</sup> s <sup>-1</sup>	$S \times P_o$ scc cm <sup>-3</sup>	$K \times 10^8$ scc cm s <sup>-1</sup> cm <sup>-2</sup> atm <sup>-1</sup>
PCTFE	He	4.9 ± 1.7	0.0076 ± 0.0030	3.7 ± 0.9
	N <sub>2</sub>			≤ 0.03 0.004–0.3 <sup>a</sup>
	O <sub>2</sub>			≤ 0.03 0.02–0.7 <sup>a</sup>
	Ar			≤ 0.11
FKM	He	5.2 ± 1.7 6.6 <sup>c</sup>	0.0084 ± 0.0034 0.023 <sup>c</sup>	4.4 ± 1.1 9–16 <sup>a,c</sup>
	N <sub>2</sub>			0.05–0.3 <sup>a,c</sup>
	O <sub>2</sub>			1.0–1.1 <sup>a,c</sup>
FFKM	He			72 ± 11 83 <sup>b</sup>
	N <sub>2</sub>			2.3 <sup>b</sup>
	O <sub>2</sub>			7.6 <sup>b</sup>

<sup>a</sup>Reference 8.

<sup>b</sup>Reference 9.

<sup>c</sup>Reference 11.

The gas flux through a saturated membrane when the source has been removed is<sup>12</sup>

$$F(x = d, t) = \frac{-2ADS P_o}{d} \sum_{n=1}^{\infty} (-1)^n \exp\left[-\frac{Dn^2\pi^2 t}{d^2}\right]. \quad (7)$$

Eqs. (5)–(7) are correct for a gasket seal if the o-ring deforms to a rectangular cross-section. The flux vanishes where the o-ring seals on the stainless steel and fused silica, so the solution is constant in that dimension, just as for an infinite two-dimensional membrane.<sup>11</sup> This is not a very good approximation for our PCTFE o-ring, which deforms with the torque approximately as shown in Fig. 1. We show in Fig. 3 a fit summing over two thicknesses, 1.5 mm and 2.5 mm, which is not a solution to the diffusion equation. We also show a fit to the fall time, which is dominated at long times by the larger thickness of the average cross-section and the first term in Eq. (7). We also show the results of a full finite element calculation including a good estimate of the geometry. We note that all fits shown do a reasonable job on the initial long delay through the bulk material before helium is detected. The result and error for diffusion and permeation in Table I reflect the geometry and its uncertainty.

## 2. Water after bakeout

After completing the S<sub>3</sub> measurements in the middle of the chamber, the main chamber was baked at 70° for 4 days. The viewports were at ~35°. PCTFE could in principle be baked to higher temperatures than FKM, but we did not test

this feature. The water level achieved after this bakeout was better than  $7 \times 10^{-11}$  Torr.

## 3. Permeation of nitrogen and oxygen

In our final vacuum system, our partial pressures for N<sub>2</sub>, O<sub>2</sub>, and Ar were less than  $4 \times 10^{-14}$  atm,  $1 \times 10^{-14}$  atm, and  $1 \times 10^{-14}$  atm, respectively. These values had shown slow improvements of an order of magnitude over 10 weeks of time; since we have no independent information on diffusion times, we cannot tell the difference between outgassing of virtual leaks and possible evolution towards an equilibrium profile of these gases in the PCTFE o-ring.

Using the known concentrations in air, and known pumping speeds (100 L/s for nitrogen and oxygen, 5 L/s for argon), and accounting for two viewports, we can deduce from the measured equilibrium leak rate and Eq. (6) upper limits on the permeation constant  $K = D \times S$  for these atmospheric gases (see Table I).

Since the partial pressures became rather small with time, it was helpful to have a check on the calibration of the RGA. A known rule-of-thumb for confinement lifetimes of atoms in magneto-optical traps (MOTs) is 1 s half-life at  $10^{-8}$  Torr.<sup>10</sup> Our MOT has reached 18 s half-lives with the two viewports attached, roughly verifying the calibration of the RGA, which is dominated by hydrogen and helium partial pressures of  $2 \times 10^{-10}$  Torr each.

We know of no other measurements of permeation nor other diffusion constants of helium and argon in PCTFE. PCTFE has been suggested as an o-ring material for transport of environmental samples, including noble gases.<sup>11</sup>

## 4. Permeability in FKM and FFKM

To check the quality of our method for measuring the helium permeation in PCTFE, we repeated the same procedure with an FKM o-ring (see Fig. 3). We found that the rise appeared similar to PCTFE. The fit to Eq. (5) was much better, from which we conclude the more pliable FKM developed a cross-section with constant thickness.<sup>11</sup> We also note the effectively larger time delay at the start for the FKM, reproduced by the calculation and attributable to its thicker constant cross-section. The diffusion parameters deduced are shown in Table I. The permeation is similar to the permeation of PCTFE, and our measurement falls below the summary of other measurements found in Ref. 8. A rate of rise test for the FKM showed a final rate of rise of 0.4 mTorr/h, similar to the PCTFE in that simple test. We did not do a full UHV test of this material, and it is possible that for some purposes two viewports with FKM could be used.

We repeated the process again for a FFKM (Kalrez 4079) viewport with the screws at 15 in.-lbs. An equilibrium helium leak rate of  $1.1 \times 10^{-5}$  Torr was reached within 0.5 min. We could not deduce  $D$  separately, but can deduce  $K$  by scaling from the equilibrium value for FKM and using Eq. (6). The large equilibrium result is consistent with previous results in the literature (see Table I), and together with the fast diffusion time make it difficult to use helium leak-check techniques on

FFKM in this viewport geometry. A rate of rise test using the FFKM showed an upper limit of 60 mTorr/h in air, which agrees within a factor of 2 with the base vacuum of the small test system and about a factor of 4 with measurements of the air permeation.<sup>9</sup>

### 5. Discussion of permeation

Inspecting Table I, we have verified that permeation of atmospheric gases through PCTFE is considerably less than through FKM, validating its choice for a UHV o-ring material. Qualitatively, the helium permeation rate is large enough, and the diffusion times fast enough, that it is difficult to distinguish leaks from permeation in normal helium leak check procedures. A RGA is a better way to check leaks for UHV use.

We note that helium diffusion through PCTFE is considerably faster than through polyimide (Kapton or Vespel), though permeation of helium and argon through PCTFE is somewhat smaller than through polyimide.<sup>13</sup> We had avoided polyimide because of its known substantial water outgassing before baking, though it has been used as a CF gasket material.<sup>3</sup>

## V. CONCLUSION

Adapting a commercial viewport design for FKM o-rings, we have demonstrated that PCTFE is a usable o-ring material for the glass-to-metal seal of UHV viewports.

The use of PCTFE o-rings reduced the stress-induced birefringence in the fused silica windows to better than  $\Delta n = -5.6 \times 10^{-6}$ . The result is circularly polarized light with  $S_3$  distorted from 0.9998 to 0.9986 in the chamber center.

The nitrogen and oxygen permeation through PCTFE in this viewport geometry was low enough to give a partial pressure of less than  $5 \times 10^{-11}$  Torr of air. The resulting half-life of our atom trap was 18 s, determined by partial pressures of nonatmospheric gases hydrogen and helium, not by air permeation.

To guarantee a seal and minimal birefringence involves some careful cleanliness and small applied torque for this relatively rigid plastic, which deforms less than fluoroelastomers. The large helium permeability of PCTFE makes it

difficult to distinguish leaks from permeation by standard helium leak checks, so an RGA is advisable for UHV work.

## ACKNOWLEDGMENTS

We thank Accu-Glass Products, Inc. for allowing our adaptation of their publicly available drawing for Fig. 1. Supported by the National Research Council of Canada through TRIUMF, and the Natural Sciences and Engineering Research Council of Canada.

- <sup>1</sup>J. A. Behr, A. Gorelov, K. P. Jackson, M. R. Pearson, M. Anholm, T. Kong, R. S. Behling, B. Fenker, D. Melconian, D. Ashery, and G. Gwinner, "TRI-NAT: Measuring  $\beta$ -decay correlations with laser-trapped atoms," *Hyperfine Interact.* **225**, 115 (2014).
- <sup>2</sup>See the NASA database at <http://outgassing.nasa.gov> for outgassing of water and other condensables from PCTFE.
- <sup>3</sup>A. Murari, C. Vinante, and M. Monari, "Comparison of PEEK and VESPEL SP1 characteristics as vacuum seals for fusion applications," *Vacuum* **65**, 137–145 (2002).
- <sup>4</sup>N. Solmeyer, K. Zhu, and D. S. Weiss, "Note: Mounting ultra-high vacuum windows with low stress-induced birefringence," *Rev. Sci. Instrum.* **82**, 066105 (2011).
- <sup>5</sup>K. J. Weatherill, J. D. Pritchard, P. F. Griffin, U. Dammalapati, C. S. Adams, and E. Riis, "A versatile and reliably reusable ultrahigh vacuum viewport," *Rev. Sci. Instrum.* **80**, 026105 (2009).
- <sup>6</sup>D. Melconian, J. A. Behr, D. Ashery, O. Aviv, P. G. Bricault, M. Domb-sky, S. Fostner, A. Gorelov, S. Gu, V. Hanemaayer, K. P. Jackson, M. R. Pearson, and I. Vollrath, "Measurement of the neutrino asymmetry in the  $\beta$  decay of laser-cooled, polarized  $^{37}\text{K}$ ," *Phys. Lett. B* **649**, 370 (2007).
- <sup>7</sup>A. A. Studna, D. E. Aspnes, L. T. Florez, B. J. Wilkens, J. P. Harbison, and R. E. Ryan, "Low retardance fused quartz window for realtime optical applications in ultrahigh vacuum," *J. Vac. Sci. Technol., A* **7**, 3291 (1989).
- <sup>8</sup>R. N. Peacock, "Practical selection of elastomer materials for vacuum seals," *J. Vac. Sci. Technol.* **17**, 330 (1980).
- <sup>9</sup>DuPont Performance Elastomers data sheet, Reorder No. KZE-H68254-00-F0203.
- <sup>10</sup>A. M. Steane, M. Chowdhury, and C. J. Foot, "Radiation force in the magneto-optical trap," *J. Opt. Soc. Am. B* **9**, 2142 (1992); D. E. Fagnan, J. Wang, C. Zhu, P. Djuricanin, B. G. Klappauf, J. L. Booth, and K. W. Madison, "Observation of quantum diffractive collisions using shallow atom traps," *Phys. Rev. A* **80**, 022712 (2009).
- <sup>11</sup>P. Sturm, M. Leuenberger, C. Sirignano, R. E. M. Neubert, H. A. J. Meijer, R. Langenfelds, W. A. Brand, and Y. Tohjima, "Permeation of atmospheric gases through polymer O-rings used in flasks for air sampling," *J. Geophys. Res.* **109**, D04309, doi:10.1029/2003JD004073 (2004).
- <sup>12</sup>W. G. Perkins, "Permeation and outgassing of vacuum materials," *J. Vac. Sci. Technol.* **10**, 543 (1973).
- <sup>13</sup>S. J. Schowalter, C. B. Connolly, and J. M. Doyle, "Permeability of noble gases through kapton, butyl, nylon, and "SilverShield"," *Nucl. Instrum. Methods Phys. Res., Sect. A* **615**, 267–271 (2010).